”Alexandru Ioan Cuza” UNIVERSITY, IAŞI
FACULTY OF PHYSICS

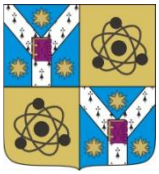

Dragoş-Ioan RUSU

CONTRIBUTIONS TO THE STUDY OF ELECTRICAL AND OPTICAL PROPERTIES OF ZnO THIN FILMS

-Summary of PhD Thesis-

Scientific Coordinator,
Professor Dumitru LUCA, PhD

- June 2013 -

”Alexandru Ioan Cuza” UNIVERSITY of IAŞI
RECTOR

No. ...../.....

Mr / Ms

We bring to your attention that on 07.06.2013, 10 am, in Room L1, Mr. **Dragos-Ioan Rusu** will support in public session, the PhD Thesis with the Title

”Contributions to the study of electrical and optical properties of ZnO thin films”

Doctoral Committee has the following structure:

President:

Professor Sebastian Popescu, PhD
Dean of Faculty of Physiscs, „Alexandru Ioan Cuza” University of Iaşi

Members:

Professor Dumitru Luca, PhD (scientific coordinator)
Faculty of Physiscs, ”Alexandru Ioan Cuza” University of Iaşi

Professor Ştefan Antohe, PhD
Faculty of Physics, University of Bucharest

Professor Victor Ciupină, PhD
Faculty of Physiscs, ”Ovidius” University of Constanţa

Professor Diana Mardare, PhD
Faculty of Physiscs, ”Alexandru Ioan Cuza” University of Iaşi

I wish to express gratitude to Prof. Univ. Dr. Dumitru Luca, scientific leader of the thesis, for his goodwill, professionalism and support demonstrated throughout the entire period of carrying out the research and development work.

Also I wish to express thanks to members of the research in physics from the State University of Moldova, University "Alexandru Ioan Cuza" from Iasi and in the same time to colleagues within the University ”Vasile Alecsandri" of Bacau, for their collaboration in obtaining and interpreting experimental results.

TABLE OF CONTENTS

INTRODUCTION

Research in the field of physics semiconductor materials have gained a special large-scale during the past two decades. The results of such research have contributed to the development of modern technologies and high-performance preparation of new materials, structures and features of great interest, as well as in the development of equipment and devices that are used with success in modern technique.

The zinc oxide belongs to the transparent and conducting oxide semiconductor group, with a range of major features, such as: chemical and thermal stability high coefficient of transmission high (75-95 %) in the field visible, high band width prohibited (eg 3.34 EV), high electrical conductivity, etc. To these it must be added the fact that zinc is found in large quantities in nature and has a low cost.

Among the problems which have not yet found resolution include: the preparation of samples with a composition as close as possible to the stoichiometric (reducing the concentration of zinc atoms in excess), the discovery of dopants that provide p-type conduction layer, to obtain preferred orientation of crystallites for layers with thicknesses greater etc. Under these circumstances, it would be able to prepare and heterojunction semiconductor junctions.

The paper studies the structure and electrical properties, optical and photoluminescence of the thin film of zinc oxide prepared by two methods: oxidation of thin layers of zinc obtained by thermal evaporation in vacuum and sputtering in magnetron system. There have been laid down for the preparation of homogenous sample, adhering to the support structure and stable properties.

Work material is grouped into five chapters preceded by an introduction, a section containing research findings and a bibliography with 167 references.

Note: Summary of the thesis was kept numbering of chapters and paragraphs, as well as that of figures, tables and references as indicated.

CHAPTER 1

CURRENT STATE OF RESEARCH ON THE STRUCTURE AND PROPERTIES OF SEMICONDUCTOR ZNO THIN FILMS

§1.1 General considerations. Research news

§ 1.1 General considerations. Research news

Expanding the range of applications in semiconductor physics was determined by using oxide semiconductor materials for making solid devices with high performance. The need to broaden the temperature range in which these devices are used to intensify investigations required transport properties, optical and photoelectric properties of oxide materials, which are irreplaceable in high temperatures [1-7].

In this paper, we study the electrical and optical properties of thin films of zinc oxide (ZnO), pure and doped with Sb and Al, obtained by: (a) thermal oxidation of zinc thin films (deposited by thermal evaporation in vacuum) and (b) reactive sputtering.

§1.2 Oxide semiconductors. General features.

Oxides which possess typical semiconductor properties are called *oxide semiconductors*. The electrical conductivity of oxides varies very widely, ranging from high values characteristic of metals (such as oxides: SnO2, In2O3, ZnO, CdO, etc..) to values characteristic of insulators (Bi2O3, TiO2, Al2O3, SiO2, etc.). [9 -11].

Many applications are based on some important features of zinc oxide, such as: high chemical and thermal stability, wide band gap (Eg> 3.0 eV), electronic transition-band direct band, low electrical resistivity, a high degree of orientation of crystallites in thin films [10,13,14].

§1.6 Techniques for the preparation and study of the properties of the semiconductor ZnO crystals

The vast majority of currently available experimental data relating to the properties of the ZnO were obtained studying the samples in the form of thin layers.

Table 1.1 Physical sizes characteristic of ZnO crystals [16.20-22].

The physical size	Value and unit of measure
Molar mass	81,4084 g/mol
Density (mass) at 20 ° C	5,42 g/cm^3
Melting point	1975 °C
Boiling point	2360 °C
Solubility (at 30 ° C) water	0,16 mg/100ml
Type crystal structure	würtzit (hexagonal)
Network parameters	a=3,249 Å (side of hexagon), c=5,206 Å (hexagonal prism height)
Band gap width, E_g (la 300 K)	3,37 eV
Band gap variation with temperature	E_g=3,34 - T/1250 (eV)
The refractive index (for λ=5893 Å)	2,068
Relative permittivity	8,3

§1.8 Methods for the preparation of thin films of polycrystalline ZnO

Among methods commonly used for preparing thin films of ZnO we mention: thermal evaporation under vacuum, spray deposition, spray pyrolysis, sol-gel method, chemical deposition from the vapor phase, thermal oxidation of the zinc layers, etc.

Methods for preparing semiconductor ZnO thin films can be grouped into two categories: physical methods and chemical methods [24,25]. The first group includes methods relating to the condensation of the gaseous phase. This group includes, inter alia: vacuum thermal evaporation, cathodic sputtering, the vapor phase reaction (epitaxial growth), oxidation reactions etc. [11,24,25].

After obtaining the thin zinc layer, it is oxidized in air at temperatures above 400 * C [10,24,27] and zinc oxide is obtained [9,27,28]. By this method it can be obtained uniform layers of ZnO with a sufficiently high deposition rate (0.1-10 * m / min.) [11,24].

CHAPTER II

EXPERIMENTAL METHODS

§2.1 Introduction

ZnO thin films studied in this work were obtained by two methods: (a) thermal oxidation of zinc thin films, deposited in advance by thermal vacuum evaporation and (b) Reactive Sputtering (DC) in magnetron configuration.

For this purpose were used equipments from the Laboratory of Semiconductor Physics at the Faculty of Physics, "Alexandru Ioan Cuza" University of Iasi and from the Research Laboratory at the "Vasile Alecsandri" University of Bacau. To study the crystalline structure of the thin films were used: diffractometer DRON-3 from the Laboratory of Structural Snalysis ("Alexandru Ioan Cuza" University), photoelectron spectroscopy X (X-Ray Photoelectron Spectroscopy XPS, PHI-Probe Verso 5000) and the microscope AFM, NT-MDT Solver Pro within the Laboratory of Plasma Physics ("Alexandru Ioan Cuza" University).

§2.2 Obtaining thin films by vacuum thermal evaporation method

The thermal evaporation method, followed by condensation under vacuum on a solid substrate, may be used, in principle, to any single solid, but also for several oxides (CdO, Sb2O3 etc) [29,31,77,85,86] or binary compounds (CdS, CdTe, ZnSe, ZnTe) [82,83,87,88].

We have used the thermal evaporatio in vacuum method for the deposit of both pure and doped layers of zinc, which were then oxidized, as well as for the deposit of metal electrode.

Most of the samples were obtained using the quasi-closed volume technique [87]. Within this method, the deposit is carried out in a much smaller volume than the volume of the deposition chamber.

Evaporator temperature was measured with a thermocouple Pt / PtRh and could vary between 700 K and 1500 K. The substrate temperature during deposition, *Ts*, was measured with a thermocouple Fe-Constantan (or a thermocouple NiCr / NiAl) and could be fixed to a certain value by means of a special device provided with two temperature limiters that set for the minimum value and another maximum.

A series of samples of zinc layers have been produced with the deposit system VUP-5 [89] (Fig.2.7), which has higher performance, but in principle has the same components and the same mode as the system UVH - 70A-1. With this system you can make deposits also on inclined supports.

To study the optical properties of ZnO thin films were drawn transmission spectra in the spectral range 300-1700 nm. We used a UV-VIS spectrophotometer type ETA-OPTIK Flag and QPM II spectrophotometer (Carl Zeiss Jena).

Fig.2.8 Spectrophotometer type ETA-OPTIK Flag.

Optical parameters of the investigated layers were determined using transmission spectra.

§2.4 Thermal oxidation of zinc thin films

In contact with the atmosphere and in the presence of water vapor from the atmosphere, the free surface of most metals is coated with a thin layer of oxide. For some metals (Al, Sn, Zn etc) oxide layer (Al2O3, SnO2, ZnO etc.) may be a protective layer, but for others (eg iron) oxidation can produce a metal etching [1.7, 10,27]. This process is the basis for the preparation of thin films of oxide by oxidation of the metal layer. Thin layers of SnO2, In2O3, ZnO etc. can be obtained by this method [1,10,22]**.**

In this thesis, zinc metal layers (obtained by thermal vacuum evaporation) were subjected to thermal oxidation in dry open atmosphere. Under the conditions used by us, using a mechanism to increase the oxide layer of the type used for silicon dioxide (SiO2) can be found that the number of embedded oxide molecules per unit volume of the oxide is about 2.2 • 1022 cm dry oxidation -3 to 4.4 • 1022 cm-3 for the wet oxidation.

Orientation of the crystallites in the layer of zinc metal influences the rate of oxidation, whereas, for certain crystallographic directions, the oxidation takes place differently. The oxidation reaction of Zn-ZnO interface depends on the arrangement of chemical bonds in that direction [10,22]. Elucidation of these issues is made using experimental samples as single crystals. Many experimental data are only for the oxidation of silicon [27]. For zinc oxidation states laws literature describe this process.

As a result of the oxidation there is a redistribution of the impurities in the layer. This process involves a phenomenon of diffusion of impurities, caused by the high temperature at which the oxidation takes place [37,38,39].

§2.5 Determination of layer thickness. Deposition rate

In this thesis, to determine the thickness of zinc and ZnO thin films, we used interferometric method [24,68] which is based on the phenomenon of interference of two beams of monochromatic radiation that is reflected on the surface layer and the support, the place where the layer has a thickness equal to the level, obtained by scraping it.

§2.6 Study of the structure of ZnO thin films by electrical microscopy

The structure of Zn and ZnO thin films, prepared by us, was studied by X-Ray Diffraction (XRD), Transmission Electron Microscop (TEM) and Scanning Electron Microscopy (SEM).

§2.7 The study of thin films using surface topography atomic force microscopy

The study of surface morphology of ZnO thin films was performed using an atomic force microscope in the endowment of the "Vasile Alecsandri " University of Bacau.

In order to measure various properties such as roughness, thickness, etc., the atomic force microscope is equipped with a cantilever having a top placed very close to the surface study. The morphological analysis of the surface can be made on very small areas, because the deflection's actuator which moves the top in the three directions (x, y, z) is limited to a few μm [59,93,94].

Using AFM technique, there were analyzed using data acquisition software package, automatic transmission and processing, WinScan.

§2.8 Measurement of electrical conductivity of ZnO layers and study of its dependence on temperature

The vast majority of the experimental data about electrical conductivity or electrical resistivity of the ZnO layers were obtained from measurements carried out by means of the two current electrodes.

Using the four electrode method (probe) is not suitable for thin film, because its limited to the surface of the existence of a space charge layer which greatly affect the measurement accuracy.

Measuring the electrical resistance and its dependence on the temperature was performed using a test device shown schematically in Fig.2.14.

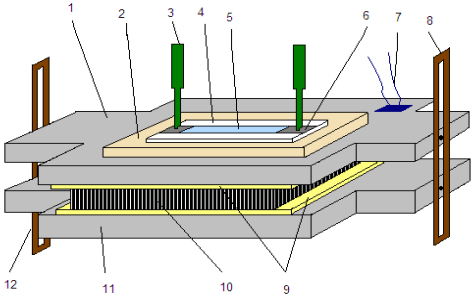

Fig.2.14 The device for measuring the electrical conductivity of the layer of ZnO and its temperature dependence.

§2.9 Obtaining thin films in planar-type magnetron systems

Sputter facility is used, at present, in the Laboratory of Physics Research Collective at "Vasile Alecsandri" University of Bacau. The layer thickness can be measured during deposition, by the interferometry method described in detail in [24,25].

CHAPTER III

THE STRUCTURE OF ZnO THIN FILMS INVESTIGATED

§3.1 General considerations

The study of thin films structure have a great importance, both to explain the physico-chemical properties of these layers, as well as their possible applications. Characterization of Zn and ZnO pure thin films studied in this thesis and the doped with Al and Sb, was performed using the following methods: X-ray Diffraction - Technique (XRD), Scanning Electron Microscopy (SEM), atomic force microscopy (AFM), X-ray Photoelectron spectroscopy (XPS) [59.109-112].

§3.2 The analysis of zinc and ZnO thin films by X-ray diffraction

To establish the X-ray diffraction (XRD patterns) we used a DRON-2 diffractometer upgraded. Recording parameter values of the diffraction were as follows: acceleration voltage, U = 26 kV; anode current intensity, I = 20 mA, wavelength of X-rays, $\lambda CuK\alpha = 1.5404$ Å.

For the analysis of several layers was used, also, the SHIMADZU diffractometer 6000, with the following recording parameters: accelerating voltage, U = 40 kV anodic current intensity, I = 30 mA..

With both devices (within the Laboratory of structural analysis at "Alexandru Ioan Cuza" University of Iasi) were drawn for diffraction angles 2θ in the range 20 ° -80 °.

§3.3 Preparation of thin films of pure and doped zinc

In this study were investigated doped ZnO thin film (obtained by thermal oxidation of the layer of zinc and by reactive sputtering), as well as some layers of ZnO doped with Sb and Al.

Aluminum-doped ZnO layers were used for the construction of photovoltaic modules such as ZnO: Al/GaSe/In2O3 and for the investigation of absorption and photoluminescence spectra at low temperatures.

In Table 3.1 are listed the conditions for the preparation of coatings studied.

In Fig.3.1 are presented two typical diffraction pattern: one for a thin layer of zinc deposited by thermal evaporation in a vacuum and the other for the same layer after oxidation. Thermal vacuum evaporation deposition was performed under the following conditions: evaporator underlying distance was 8 cm, evaporator temperature, *TEV = 700 K*, deposition rate, *rd = 13 to 14 Å / s*, substrate temperature during deposition, *Ts = 300 K*. The XRD patterns

show that the zinc layer is polycrystalline and has a preferred orientation of the plane (002) parallel to the support surface.

Since it was found that these parameters ensure the layers, adhesion to the substrate, with constant thickness, we chose to use in all cases where the layers were deposited Zn, Zn and Al, Zn and Sb. Where we used otherwise, these will be listed separately.

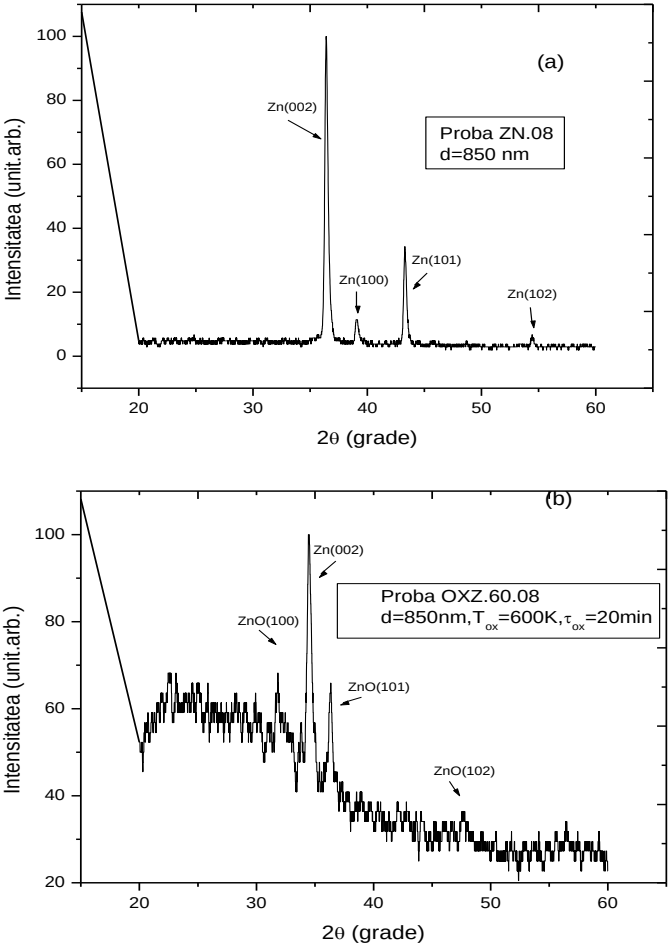

Fig.3.1 The X-ray diffraction of a thin layer (a) of zinc (sample ZN.08), (b) zinc oxide (sample ZN.60.08) is obtained by oxidation of the layer (a). The oxidation temperature, Tox = 600 K, during the oxidation, tox = 20 min. [103]

Table 3.1 Conditions for preparation of thin films studied

Thin	Preparation	Nature of	Type of	The material	Research

layer	method	the support	structure	placed in the evaporator	conducted
ZnO	Thermic oxidation	Amorphous glass, SiO_2	Würtzit	Polycrystalline powders of Zn	- Structure - Electrical properties - Optical properties
ZnO	Sputtering	Amorphous glass	Würtzit	Zn Disk	- Structure - Electrical properties - Optical properties
ZnO dopat cu Al	Thermic oxidation of Zn:Al layers	Amorphous glass, SiO_2	Würtzit	Polycrystalline powders Zn și Al	- Electrical properties - Optical properties - Fotoluminisc
ZnO dopat cu Sb	Thermic oxidation of Zn:Sb layers	Amorphous glass	würtzit (partially amorphous)	Polycrystalline powders of Zn și Sb	- Structure - Optical properties

§3.4 The conditions of production and oxidation of the thin layer of zinc

Zn thin films with thickness of 200-2000 nm were deposited by thermal vacuum evaporation with a deposition rate of 14 nm / s. These are polycrystalline and have a hexagonal compact structure [114,118].

The layers of Zn were subjected to oxidation at a temperature between 600 and 850 K, being maintained at that temperature for the time intervals (for oxidation), tox = 10-120 min. Subsequently layers were cooled to room temperature at a rate of about 10 K / min. XRD patterns have shown that these conditions cause complete oxidation of the zinc layer.

§3.5 The crystal structure of ZnO layers

Thin layers of Zn investigated in this thesis were prepared prior to the oxidation, by means of thermal evaporation in vacuum, using the polycrystalline Zn powder (Merck, 99.99%) and sputtering in the magnetron system. ZnO layers obtained in the end are also polycrystalline and a Wurtz-type structure (hexagonal) (Fig.3.1 (b)).

It was observed that with increasing duration of oxidation, the intensity peaks (100) and (101) show an increase.

The structure of ZnO layers was examined by identifying and indexing maxima (peaks) of the diffraction performed by X-ray diffraction,

and their position in the diffractogram identified with indications of JCPDS files (Joint Committee for Power Diffraction Standards) [114-118].

As radiation source was used anticatod copper, line CuK_α being selected by the filter absorption of aluminum, with a thickness gauge. Corresponding wavelength is $\lambda = 1.5404$ Å.

The structural analysis made on the basis of the diffraction of the ZnO layer (Fig.3.1-3.5) confirm that these layers have Wurtz-type hexagonal structure with a strong texture in the planes (002) parallel to the support surface. Preferential orientation of crystallites of ZnO layer planes (002) parallel to the substrate surface is indicated by the high intensity of the diffraction peak identified at $2\theta = 34.45^\circ$ Fig. 3.1).

Standard diffraction peaks corresponding angles for Zn and ZnO and respective Miller indices were taken from the relevant ASTM (American Society for Testing Materials), published by JCPDS [116 117].

Fig.3.4 presents the diffractogram of four layers of ZnO with increasing thickness, oxidized at a temperature of 600 to 700 K, at intervals of 20 and 30 minutes.

It can be seen that, under the conditions of oxidation mentioned, the layers have been completely oxidized, the characteristic peaks are not observed in crystals of zinc. You can find some general features of the structure of deposited layers in this set of experiments:

- All the layers are polycrystalline and a Wurtz-type structure;
- Crystallites have a preferred orientation of the planes (002) parallel to the surface of the deposit;
- In the case of the lower layers thick (d = 780 nm, Fig.3.4 (a)), this orientation is the majority. It may be admitted that, in the early stages of growth of the crystallite layer is thus formed;
- With increasing thickness, (d = 900 nm, Fig.3.4 (b)) is observed an amorphous phase. The direction of orientation of the crystallites of the planes (002) parallel to the film surface is maintained, but the appearance of the crystallites is also found in other orientations, (100) and (101);
- The subsequent increase in the thickness (Fig.3.4 (c)), there are standard guidelines crystallites with (100) and (101) parallel to the film surface and reduces the weight of the amorphous phase;
- With the increase of the thickness (Fig.3.4 (d)) it decreases the degree of texturing.

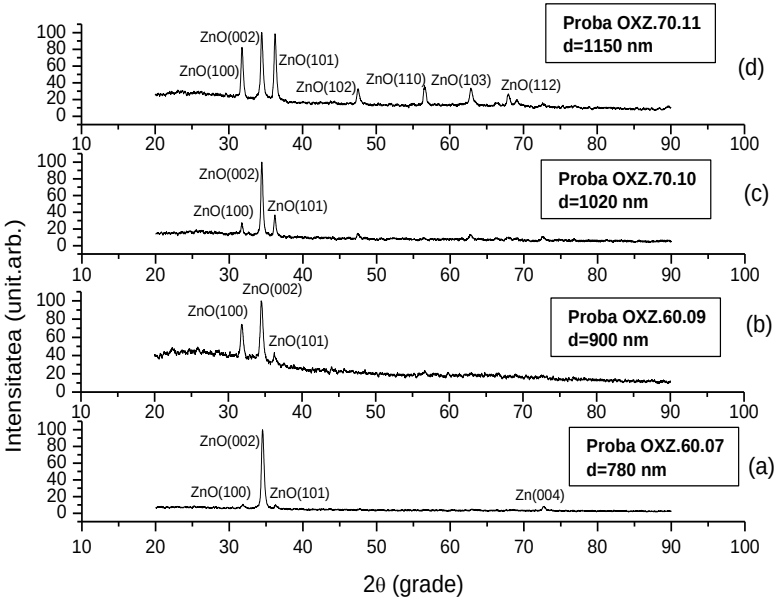

Fig.3.4 X-ray diffraction of the ZnO thin with different thicknesses.

As noted above, the layers have a preferred orientation of crystallites, the peak corresponding diffraction planes (002) are very pronounced. The peaks in the diffraction pattern also indicates that the planes (100), (101) and (102) are, for some groups of crystallites parallel to the surface of the support. Using the characteristics peaks respective network parameter values were calculated (Table 3.1).

For large thickness of the film the oxidation remains incomplete. Thus, the ZnO layer of a thickness of 11.5 μm, obtained by oxidation at a temperature of 800 ° C for one hour, indicate the presence of diffraction peaks characteristic only of zinc. These results can be attributed to the presence of Zn micro crystallites remaining unoxidized or diffusion effect of zinc atoms on the surface of the crystallites become excessive.

In conclusion, we can say that the thermal oxidation of zinc layers is a viable alternative to obtain ZnO layers if the layer thickness is not exceeding 1 μm zinc and oxidation temperature is not too high (T <700 K).

Since oxidation takes place in the open air, we assume that too high temperature leads to a pressure drop of oxygen in the vicinity of the layer of zinc and as a result the layer obtained is with lack of oxygen. Excess Zn atoms can diffuse to the surface of the crystallites, forming microcrystalitesl.

Crystallite orientations with the *c* axis of the hexagonal unit cell perpendicular to the film was observed in the case of reactive sputter deposited layers, as we shall see in

the next section. Neither in this case, is not observed the presence of oxidized zinc atoms.

Table 3.1 Some characteristic parameters of studied layers.

Sample	*d* (nm)	r_d (Å/s)	T_s (K)	T_o (K)	τ_o (min)	2θ (deg.)	(*hkl*)	d_{hkl} (Å)	*a* (Å)	*c* (Å)
OXZ.60.07	780	15	300	600	20	34.36	002	2.604	3.252	5.193
OXZ.60.09	900	14	300	600	20	31.74	100	2.803	3.241	5.182
						34.42	002	2.592	3.231	5.192
OXZ.70.10	1020	13	300	700	30	31.70	100	2.816	3.266	5.217
						34.41	002	2.603	3.251	5.208
OXZ.70.11	1150	14	300	700	30	31.68	100	2.808	3.247	5.196
						34.38	002	2.607	3.239	5.204

d - thickness of layers; r_d, deposition rate; T_s, substrate temperature during deposition, T_{ox}, oxidation temperature; t_{ox}, oxidation time, θ, Bragg angle, (*hkl*) planes with Miller indices *h*, *k*, *l*; d_{hkl}, the distance between the planes (*hkl*), *a* and *c*, the network parameters of Wurtz-type hexagonal structure.

§ 3.6 Structure of ZnO layers prepared by sputtering

In Fig.3.8 is shown a diffractogram corresponding to the ZnO layer deposited by sputtering under the conditions specified in § 2.13. It is noted the preferred orientation of the plane (002) parallel to the film surface occurs as in the case of films studied in § 3.5.

Here we find a contrast to the layers prepared by thermal oxidation. The samples obtained by spraying maintain the orientation of the crystallites of the planes (002) parallel to the surface of the support even for large thicknesses. On the ZnO layer prepared by thermal oxidation with increasing thickness is observed, and also other peaks corresponding to planes (101), (100), (102), etc.

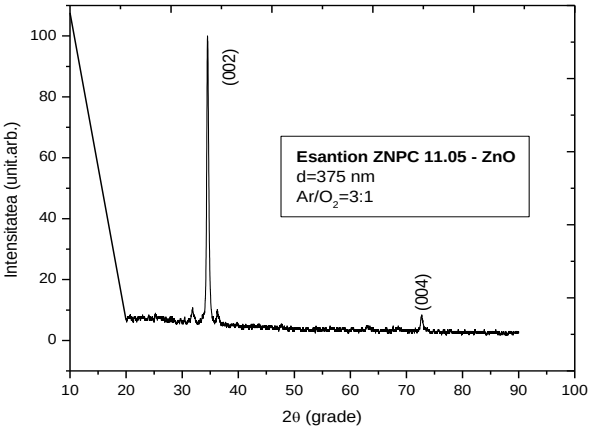

Fig.3.8 The X-ray diffractogram obtained for sample ZNPC.11.05-ZnO

§3.7 Texture coefficient

Texturing is the orientation of crystallographic planes after various directions under the influence of the preparation or action of external factors. *The texture* can be expressed in terms of *texture coefficient* [12,106], which is calculated from the equation

$$TC(hkl) = \frac{I(hkl)/I_0(hkl)}{N^{-1}\sum_N \left[I(hkl)/I_0(hkl)\right]} \tag{3.5}$$

where $I_0(hkl)$ is the intensity of the peak or standard (ASTM specified in the schedule), $I(hkl)$ is the peak intensity of the diffraction experimental results determined respectively, and N is the number of diffraction peaks considered [59].

The values of $TC\ (hkl)$ are given in Table 3.2, the planes (100), (002) and (101).

Table 3.2 Oxidation conditions and texture coefficient values for thin layers of ZnO [103].

Sample	d(nm)	T_{ox}(K)	τ_{ox}(min)	$TC(hkl)$ (%)		
				(100)	(002)	(101)
OXZ.60.07	780	600	20	0.23	2.49	0.56
OXZ.60.09	900	600	20	1.35	2.03	1.08
OXZ.70.10	1020	700	30	1.23	2.38	1.19
OXZ.70.11	1150	700	30	1.47	2.16	1.30

d - the layer thickness, T_{ox} - temperature oxidation; τ_{ox} - during the oxidation; $TC_{(hkl)}$ - coefficient of texture planes of Miller indices (hkl).

§3.8 Zn-O bond length

For an ideal Wurtz network type, Zn-O bond length can be calculated using the equation [12,15,129]

$$L = \left[\frac{a^2}{3} + \left(\frac{1}{2} - U \right)^2 c^2 \right] \tag{3.6}$$

where the parameter U for the Wurtz-type networks is

$$U = \frac{a^2}{3c^2} + 0.25 \tag{3.7}$$

Data from the network parameter values determined from the diffraction of X-rays are presented in Tables 3.3 and 3.4.

Table 3.3 Values of the structural parameters for the layers studied.

Sample	D (nm)			L (nm)
	(002)	(110)	(101)	
OXZ.60.07	26.23	–	–	1.94
OXZ.60.09	30.93	28.41	28.46	1.93
OXZ.70.10	27.97	24.68	26.97	1.94
OXZ.70.11	32.21	27.68	27.37	1.93

D, crystallite size; *L*, Zn-O bond length.

For hexagonal structure with compact arrangement (with a coefficient of compactness η = 0.74), the ratio c / a = 1.633 [18.23-25] provides a compact packing of atoms, consider the tangent spheres with equal rays. If the layers of zinc which have this kind of structure, we find D / A = 1.847, which indicates that the structure that is different from an ideal HC structure.

Table 3.4 Structural characteristics of thin layers of Zn and ZnO.

Sample	Composition	d (nm)	T_{ox} (K)	τ_{ox} (min)	Type of structure	2θ (degree)	(*hkl*)	a (Å)	c (Å)
ZN.05	Zn	540	-	-	hexagonal compact	36,28	(002)	-	4,946
						39,00	(100)	2,624	-
ZNO.09	ZnO	900	600	20	würtzit	31.75	(100)	3,236	-
						34.35	(002)	-	5,218

d – layer thickness, T_{ox} –oxidation temperature, τ_{ox} – oxidation time, θ – Bragg angle, *(hkl)* – Miller indices, a și c – unit cell parameters for hexagonal compact structure Wurtz-type structure.

§3.9 Residual voltage. Stress

Typically, residual tension which arises within a thin layer can be written as [27,61]

$$\sigma = \sigma_{\text{int}} + \sigma_t \tag{3.9}$$

where σ_{int} is the voltage that occurs during deposition of the layers (due to the presence of structural defects and impurities, as well as other parameters of deposit), and σ_t is the thermal component of the voltage, which is determined by the difference between the coefficients of linear thermal expansion of the layer and the substrate [17,27].

The tensions along the *c* axis of ZnO layers can be calculated using the expression [17,58]

$$\varepsilon_2(\%) = \frac{c - c_0}{c_0} \times 100 \tag{3.10}$$

where *c* is the parameter of haxagonale cell Wurtzit for thin layers, and c_0 is the same parameter in the case of solid crystal ZnO (c_0=5.2066 Å).

Residual stress, σ, the ZnO layer is determined using the connection [17.27]

$$\sigma = \frac{2c_{13}^{\ 2} - c_{33}(c_{11} + c_{12})}{2c_{13}} \cdot \frac{c - c_0}{c_0} \tag{3.11}$$

where c_{ij} represents ZnO monocrystal elastic constants (values given in Table 3.5).

Using these values, we can write the equation (3.11) as

$$\sigma = -232.8 \cdot \frac{c - c_0}{c_0} \text{ (în GPa)} \tag{3.12}$$

Table 3.5 The elastic constants of the crystal of hexagonal system at room temperature.

Material	C_{11}	C_{33}	C_{44}	C_{12}	C_{13}	References
Zn	161	610	38,3	34,2	50,1	[119]
ZnO	209,7	201,9	42,5	121,1	105,1	[120]
ZnO	208,8	213,8	-	119,7	104,2	[121]

The microstress arising in the ZnO layers can be calculated using the equation [25,27]

$$\varepsilon = \frac{\beta_{2\theta} \cdot \cos\theta}{4} \tag{3.14}$$

where $\beta_{2\theta}$ is the half width of the diffraction peak.

For some of the samples studied, the values of ε are shown in Table 3.6.

It can be seen that if the oxidation temperature is 700 K, the stress of expansion of the layers is eliminated and the crystallinity improves.

Table 3.6. Values microstress and residual stress values for some samples studied.

Sample	(*hkl*)	*c* (Å)	ε $\times 10^{-3}$ (%)	σ (GPa)
OXZ.60.07	002	5.193	-2.6	0.605
OXZ.60.09	100	5.182	-4.7	1.094
	002	5.192	-2.8	0.651
	101	5.191	-2.9	0.675
OXZ.70.10	100	5.217	1.9	-0.442
	002	5.208	2.6	-0.605
	101	5.219	2.3	-0.535
OXZ.70.11	100	5.196	2	-0.465
	002	5.204	-0.4	0.093
	101	5.193	-2.6	0.605

c – network constant; ε - micro stress; σ - residual stress.

§3.10 Determination of crystallite sizes

The average size of the crystallites, *D*, determined in the direction normal to the diffraction planes (100), (002) and (101) were calculated using the Debye-Scherrer equation [12,62,110,111]

$$D = \frac{k\lambda}{\beta_{2\theta} \cos\theta} \qquad (3.15)$$

where λ is the wavelength of X-radiation used (for CuK_α, λ=1,5418 Å), *k* is Scherrer constant, and $\beta_{2\theta}$ is the physical half-width of the diffraction peak, for which the Bragg angle is θ.

Average crystallite size values preferentially oriented with the planes (002) are dependent on the thickness of the layers and are within the range from 24.68 to 32.21 nm. The results are shown in Table 3.7.

Scherrer constant was considered as k = 0.90 [110,125,126,152]. Equation (3.15) applies to the profile of the diffraction peaks at small angles is Gaussian [111].

With increasing layer thickness, crystallite size increases [122-124].

Table 3.7 Structural parameters for ZnO samples with different thicknesses

Sample	d(nm)	r_d(nm/s)	T_s(K)	2θ	(hkl)	D(nm)	d_{hkl}(Å)	a(Å)	c(Å)
OXZ.80.03	980	24,5	300	34,4	002	26,23	2,59	3,25	5,19
				72,6	004	25,82	2,6	3,25	5,20
OXZ.90.50	1100	22	300	31,7	100	28,4	2,8	3,24	5,18
				34,4	002	30,93	2,59	3,23	5,19
				36,2	101	28,46	2,59	3,25	5,19
OXZ.90.02	1220	20,3	300	31,7	100	24,68	2,81	3,26	5,21
				34,4	002	27,97	2,6	3,25	5,2
				36,2	101	26,97	2,61	3,25	5,21
OXZ.90.01	1350	22,5	300	31,7	100	27,68	2,8	3,24	5,19
				34,4	002	32,21	2,6	3,23	5,2
				36,2	101	27,37	272	3,25	5,19

d – sample thickness, r_d – deposition rate, T_s support temperature, θ –Bragg angle, *(hkl)* - Miller indices corresponding diffraction planes, D – crystallite size, d_{hkl} – distance between the planes with Miller indices (hkl), a şi c – lattice parameters.

§3.12 Morphological analysis of ZnO layers by AFM technique

Surfaces of ZnO layers were analyzed by atomic force microscopy (AFM) in non-contact mode. In Fig.3.10-3.14-dimensional AFM images are representative of some thin layers on the scanned area of 3.0 μm × 3.0 μm.

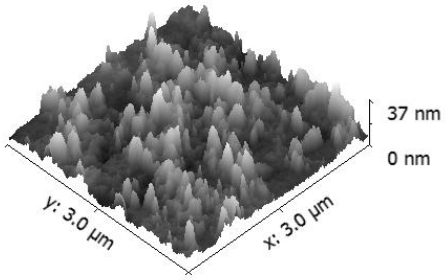

Fig.3.12 3D AFM image for sample OXZ.60.24.
(thin layer of zinc deposited on the glass substrate at a temperature T_s=300 K and oxidized at a temperature T_{ox}=700 K; oxidation time τ_{ox}=30 min.).

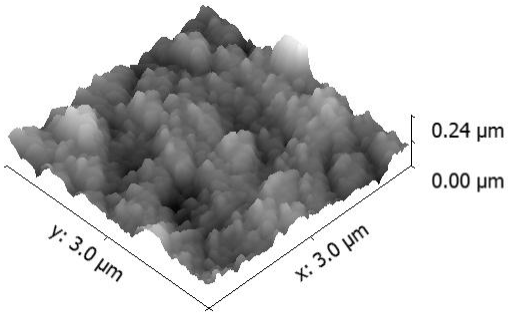

Fig.3.14 3D AFM image for sample OXZ.60.26 (thin layer of Zn, deposited on the glass substrate at a temperature T_s=300 K and oxidized at a temperature T_{ox}=750 K;oxidation time τ_{ox}=25 min.).

Surface roughness characteristics of the layers analyzed are valued using roughness parameters, among which:

- Roughness average (arithmetic mean) R_a, which is calculated as the arithmetic mean of the heights z_i measured for each grid point, the scan is performed on the surface analyzed

$$R_a = \frac{1}{n}\sum_{i=1}^{n}(z_i - \bar{z}) \tag{3.19}$$

- Mean square roughness, R_q (also noted with R_{rms} or R_{RMS}) is the average squared difference between the height z_i the sample at a point to the horizontal plane mainly and the height $\bar{z}$ on the surface of the sample.

$$R_q = \sqrt{\frac{1}{n}\sum_{i=1}^{n}(\bar{z} - z_i)^2} \tag{3.20}$$

In Table 3.8 are given values of roughness R_a şi R_q two of ZnO thin films studied.

Table 3.8 Values of the structural parameters for the layers studied.

Sample	D (nm)			L (nm)	R_a(nm)	R_{rms}(nm)
	(002)	(110)	(101)			
OXZ.60.07	26.23	–	–	1.94	108	144
OXZ.60.09	30.93	28.41	28.46	1.93	–	–
OXZ.70.10	27.97	24.68	26.97	1.94	–	–
OXZ.70.11	32.21	27.68	27.37	1.93	35	45

D, crystallite size; *L*, Zn-O bond length; R_a, average roughness; R_{rms}, mean square roughness

§3.13 XPS spectra of ZnO thin layers

In order to determine the degree of oxidation of the ZnO thin films , were drawn XPS spectra [59.127].

Layer has a thickness greater than a composition with a slight stoichiometric excess of oxygen. The thickness is less than an excess of oxidized zinc atoms. Such a composition has been found to webs prepared by other methods, and the ZnO crystals.

It can be considered that in the conditions used we obtain coatings without departure from the structure of solid material, in which is established the presence of interstitial zinc ion, in excess.

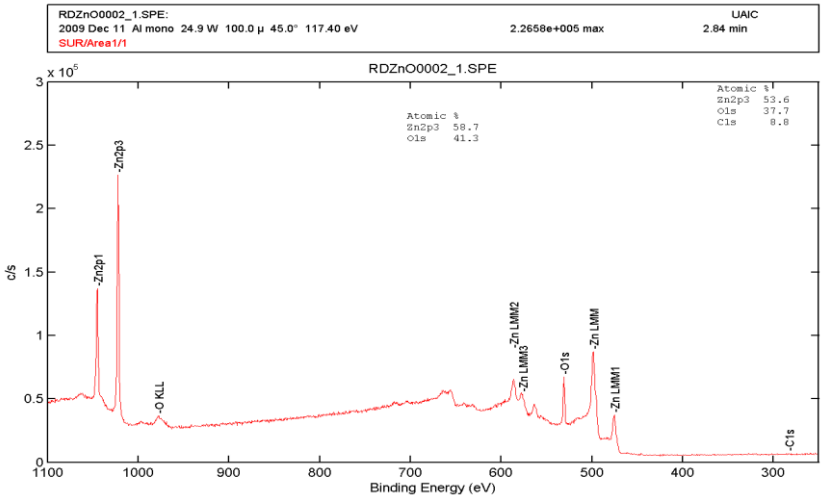

Fig.3.17 XPS spectra for sample 70.11.

CHAPTER IV

ELECTRICAL CONDUCTION IN THIN FILMS OF STUDIED ZnO MECHANISM

§4.2 Analysis of experimental data on the influence of the heat treatment on ZnO thin films

In Fig.4.1 are presented the curves $\ln\sigma = f(10^3/T)$ for the ZnO thin film prepared by thermal oxidation of the zinc layer at T = 600 K, with an oxidizing t_{ox} = 30 min. The sample was subjected to two successive both heating and cooling.

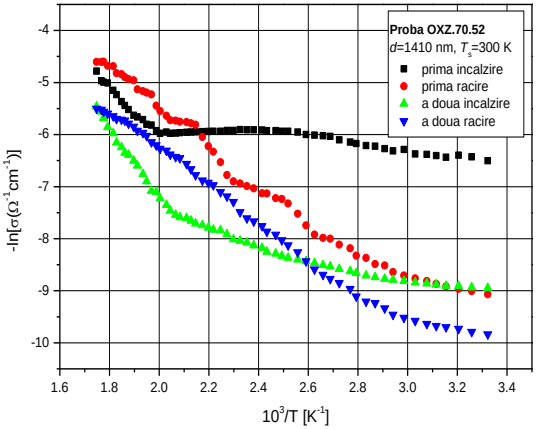

Fig.4.1 The temperature dependence of the electrical conductivity sample OXZ.70.52 - ZnO (T_s = 300 K, d = 1410 nm).

In Table 4.1 are shown the values of the electrical conductivity before the heat treatment, σ_i , and after the heat treatment, σ_f, at room temperature.

Table 4.1 The values of electrical conductivity at room temperature, before heat detratament, σ_i , and after the heat treatment, σ_f.

Sample (ZnO)	T_S (K)	d (nm)	σ_i ($\Omega^{-1}\cdot cm^{-1}$)	σ_f ($\Omega^{-1}\cdot cm^{-1}$)
OXZ.90.33	300	1500	$2{,}7\cdot10^{-3}$	$2{,}2\cdot10^{-4}$
OXZ.90.40	300	1150	$2{,}2\cdot10^{-4}$	$1{,}3\cdot10^{-5}$
OXZ.80.01	300	900	$2{,}7\cdot10^{-4}$	$1{,}3\cdot10^{-4}$
OXZ.90.30	573	930	$2\cdot10^{-5}$	$1\cdot10^{-5}$
OXZ.70.50	573	1300	$4\cdot10^{-4}$	$3{,}7\cdot10^{-5}$
OXZ.70.52	573	1410	$1{,}8\cdot10^{-3}$	$6{,}1\cdot10^{-4}$

E_{a1}, activation energy values, calculated in the first temperature range by ΔT_1 and the E_{a2}, calculated for the second temperature ΔT_2, are shown in Table 4.2.

Table 4.2 The thermal activation energy of electrical conductivity corresponding to ZnO thin films

Sample(ZnO)	T_S (K)	d (nm)	ΔT_1 (K)	E_{a1} (eV)	ΔT_2 (K)	E_{a2} (eV)
OXZ.90.33	300	1500	413-303	0,37	555-413	1,31
OXZ.90.40	300	1150	400-303	0,3	588-434	0,55
OXZ.80.01	300	900	408-303	0,7	487-458	1,08
OXZ.90.30	573	930	434-301	0,47	561-434	0,19
OXZ.70.50	573	1300	434-303	0,17	561-434	0,42
OXZ.70.52	573	1410	480-303	0,17	561-480	1,27

§ 4.3 The effects of heat treatment in vacuum

Fig.4.8 presents the results obtained for two of the samples studied (with identical preparation conditions). Zinc coatings were deposited simultaneously and the oxidation was carried out at T_o=600 K, an oxidation time of 60 minutes. The layer thickness is d=1,35 μm.

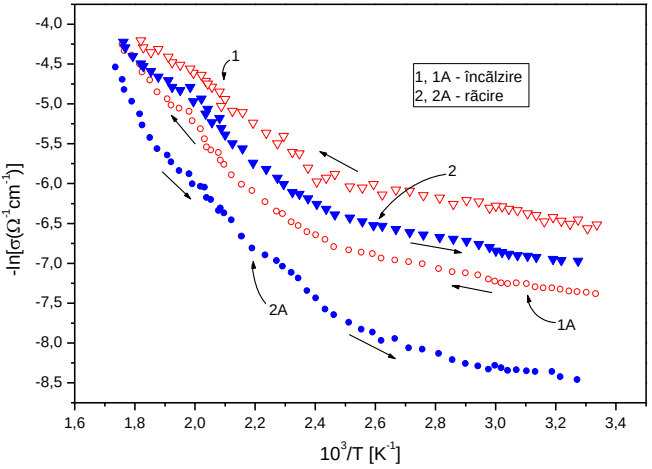

Fig.4.8 Variation with the temperature of electrical conductivity in air (curves 1 and 2) and in vacuum (curves 1A and 2A)

Following heat treatment in vacuum, the graphics $\ln\sigma=f(10^3/T)$ are removed first, indicating the effect of irreversible processes, such as elimination of absorbed and adsorbed gas, as well as excessive oxidation of Zn atoms.

Finally, repeating cycles of heating / cooling, the curves $\ln\sigma$=f ($10^3/T$) are approching and the dependencies become reversible. It can be seen that the treatment intfluence is stronger when dealing with low temperatures.

When removing the air inside the vacuum layer, the thermal conductivity increases slightly, probably influenced by the presence of oxygen.

§4.4 The mechanism of electrical conduction in thin layers polycrystalline ZnO. Compared to the Seto [73]

To explain the temperature dependence of the electrical conductivity of the samples, we used the model proposed by Seto.

The results of applying the Seto model (note that the model is known under this name, although changes brought by Baccarani et al. [74] are very important) can be formulated as follows:

1) The boundaries between crystallites play an essential role in the electrical conduction mechanism. Concentration of surface states is $1{,}7\cdot10^{12}$–$2{,}8\cdot10^{13}$ cm^{-}2 and the energy of energetic levels introduced by these states in the band gap is E_t=0,42-0,50 eV.
2) For the study layers, the crystallites are small, thus is assumed to be fully depleted of free carriers.
3) However, for layers with larger thickness, values of the activation energy in the higher temperature domain (T>500°C), are similar to $E_g/2$ (E_g bandwidth is prohibited).

§4.5 Spread carriers crystallite surfaces. Verification of the Mayada Shatzkes Model

To explain several results that we have obtained, we confront our results with a model proposed by Mayadas and Shatzkes [136].

Table 4.5 Application of the Mayadas - Shatzkes model.

R_D	l_0/L	A	σ_S/σ_0
0,1	10	1,11	0,382
0,2	10	2,50	0,228
0,3	10	4,29	0,125
0,4	10	6,67	0,103
0,5	10	10,00	0,069
0,6	10	15,00	0,047

CHAPTER V

OPTICAL PROPRIETES OF ZnO THIN FILMS

§5.2 The transmission and absorption spectra

In the following, for a series of samples were drawn three spectra [102, 106, 108]:

1. A spectrum representing the dependence of the transmission coefficient (expressed in percentage) of the wavelength (in nm) of the incident radiation normal to the layer. Optical transmission coefficient was calculated taking into account the transmission coefficient of glass-coating system and transmission coefficient of the uncoated substrate (see §2.10)

2. To calculate the absorption coefficient was used the equation [74,75]:

$$\alpha = \frac{1}{d} \ln \frac{(1-R_\lambda)^2}{T_\lambda} \tag{5.2}$$

where d is the layer thickness and R_λ and T_λ are the reflection coefficients, also the transmission coefficients , corresponding to a wavelength λ (or an incident photon energy hv). We plot the dependence α=f(hv).

3. Regarding the dependence of the absorption coefficient of the incident photon energy in the fundamental absorption band edge, are considered direct band-band transitions allowed, which respect the relation Tauc [4,5,74,153].

Fig.5.2 contains the transmission spectra for a sample subjected to heat treatment after being maintained at a temperature of 700 K, different periods of time (10 min., 15 min. and 20 min.). Deependencies $(\alpha \cdot hv)^2 = f(hv)$ for the same sample are shown in Fig.5.4 [132, 139, 140].

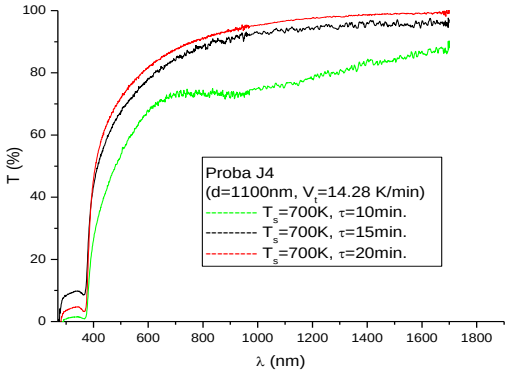

Fig.5.2 Transmission spectrum of a sample, following the heat treatment.

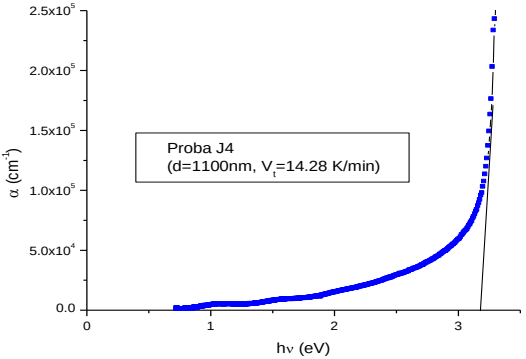

Fig.5.3 α=f ($h\nu$) dependence for the studied sample.

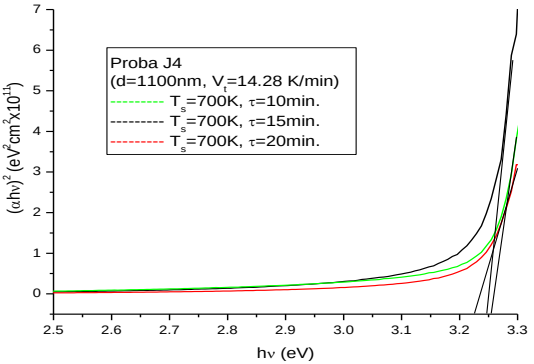

Fig.5.4 $(\alpha \cdot h\nu)^2$ = f($h\nu$) dependence for a sample subjected to heat treatment.

It can be seen that with the increase of the heat treatment at a temperature of 700 K, the edge of the transmission spectrum becomes sharper, which indicates the achieving of a correct stoichiometry and decreased concentrations of structural defects (presumably oxygen vacancies and interstitial zinc atoms).

§5.3 Absorption spectra at low temperatures

I performed a systematic study of the phenomenon of absorption of ZnO layers in low temperatures. Crystallites had a strong orientation planes (002) parallel to the substrate surface (Fig.5.9)

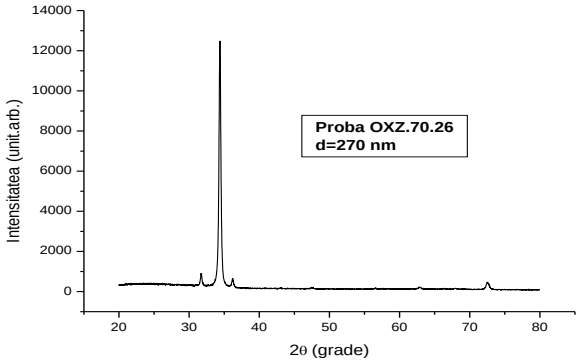

Fig.5.9 Diffractogram OXZ.70.26 sample (ZnO).

Typical absorption spectra from 78 K to 293 K are shown in Fig.5.10 and 5.11. At a temperature of 78 K absorption occurs with the formation of excitons. It is known that the transition of an electron from the valence band to the conduction band is equivalent to ionize an atom of the semiconductor crystal. This process occurs when atomic energy is transmitted at least the width of the band gap. If the energy imparted is less than the width atom band gap, the electron remains bound to the atom, the latter is in an excited state. These excited states correspond to energy levels in the band gap, close to the conduction band.

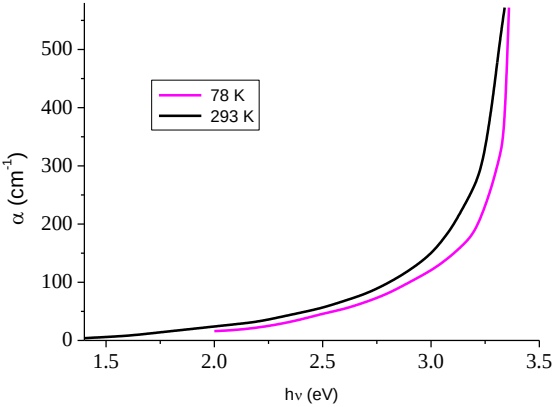

Fig.5.10 Absorption spectra of a thin layer of ZnO at a temperature of 293 K and 78 K

Such excited states are called excitons [58,74,75,142]. Excitation energy can be transmitted from one atom to another, a process equivalent to an excited atom move through the crystal.

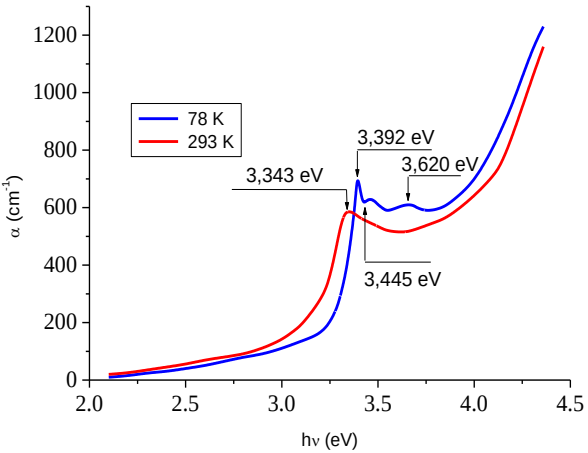

Fig.5.11 Absorption spectra of a ZnO thin film at a temperature of 293 K and 78 K.

The absorption spectra of the film at a temperature of 293 K result in a value of 3,343 eV absorption band, and at a temperature of 78 K the maximum moves to the high energy and it is converted into three bands corresponding to the energy of 3,392 eV, 3,445 eV and 3,620 eV [102,104,106].

The energy bands $h\nu_1$=3,392 eV and $h\nu_2$=3,445 correspond to the large exciton radius states n=1 şi n=2. We determine the band gap width as E_g=3,459 eV at T=78 K. The exciton binding energy is equal to 67 meV.

§ 5.5 Development of photovoltaic modules based on ZnO layers

Photovoltaic effects, underlying the construction of solar cells, are particularly addressed extensively in the past decades [47,74].

We studied the mechanisms of generation / recombination and transport of nonequilibrium charge carriers in heterojunction ZnO/In_2O_3/InSe:Cd. We also analyzed the current-voltage characteristics and spectral characteristics of short-circuit photocurrent [5,24,74].

The crystals of indium selenide (InSe), prepared using the Bridgman method, have been doped with Cd, to give them a p-type conduction. The layers of ZnO and In_2O_3 were obtained by air oxidation of the zinc and indium metal layer, deposited by thermal evaporation in vacuum. Layers of ZnO are doped with Al (1.5 at%).

Regarding the recent results [147] achieved by a group where I also belong, we mention:

- The edge of the strip for absorption of InSe is determined indirectly by participating exciton transitions;
- Spectral characteristics of photocurrent has a maximum for $h\nu$=1,5 eV;
- InSe diffusion length is between 0.9 μm and 1.8 μm;
- We discussed the current-voltage characteristics of ZnO:Al/In_2O_3/p-InSe:Cd [147].

These results are of great interest and recommends further research to increase the conversion efficiency of these systems.

§ 5.7 Photoluminescence of ZnO thin films

We studied the spectral dependence of photoluminescence for ZnO layers at temperatures of 78 K and 293 K. The samples were provided with gold electrodes. These spectra are shown in Fig.5.13.

As can be seen, the spectrum at temperature of 293 K has a peak at 3,28 eV (a) and a band composed of four sub-bands, with maximum of 2,47 eV, 2,35 eV, 2,75 eV and 2,10 eV. It can be assumed that the band (a) is obtained by radiative recombination of excitons with emission of phonons with energy of 60 meV. This process is determined by the moving belt (a) to 60 meV at lower energy as compared with that of the peak of the absorption spectrum.

The corresponding band energy of 2,47 eV is due to the recombination of the gaps of the valence band with the electrons of the corresponding energy level of ionized oxygen vacancies. The band of 2,75 eV is determined by radiative recombination of electrons from shallow donor levels with the gaps in the valence band.

At the temperature T = 78 K photoluminescence spectrum structure remains. It has a maximum at 2,28 eV determined by the presence of impurity levels and a band at 2,10 eV due to recombination of electrons from the conduction band with gaps occupying the energy levels introduced by the double ionized oxygen vacancies. Bands located at 3,364 eV and 3,338 eV arise from free exciton disappearance, who are in state n = 1, with the emission of optical phonons.

In order to determine the nature of the 3,364 eV band, we analyzed the temperature dependence of the maximum intensity. It is found that the peak is due to exciton annihilation located on vacancies oxygen levels [141].

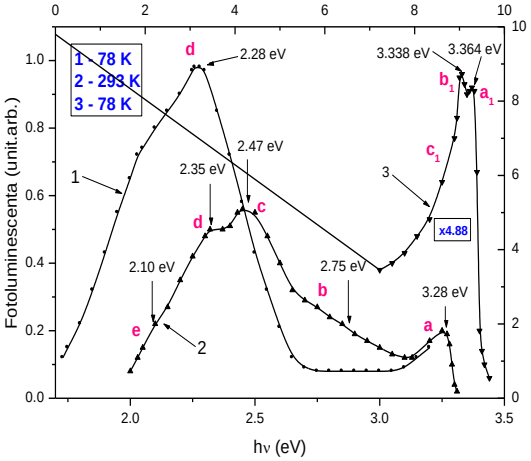

Fig.5.13 Photoluminescence spectra for a ZnO layer, supported on SiO_2**.**

§ 5.8 Antimony doping influence on the properties of the thin layers of ZnO

There were also submitted several layers with mixed Zn and Sb_2O_3. It appears that a significant amorphous phase is obtained immediately after deposition (Fig.5.14). If the sample is subjected to heat treatment, it is achieved a characteristic peak for ZnO planes (002) and several characteristic peaks of cubic Sb_2O_3 (Fig.5.15).

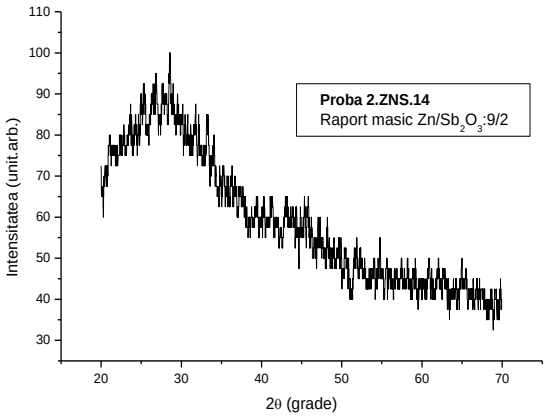

Fig.5.14 Diffractogram of the 2.ZNS.14 sample (thin layer of Zn and Sb_2O_3) immediately after deposition, without thermal treatment.

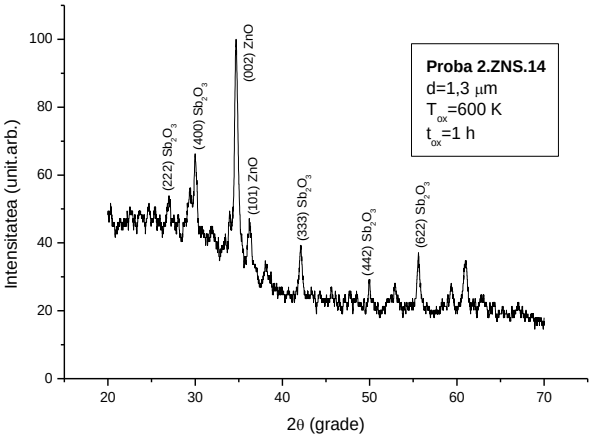

Fig.5.15 Diffractogram 2.ZNS.14 sample (thin layer of Zn and Sb2O3) after the heat treatment.

The structure of the Zn/Sb și Zn/Sb_2O_3 was studied, the samples were subjected to thermal treatments similar to those performed for Zn layers. Presumably Sb_2O_3 crystallizes and has no preferred orientation of crystallites (there are many peaks characteristic of cubic Sb_2O_3), and the ZnO crystallites were oriented with the plane (002) parallel to the support.

Regarding the electrical properties, there is a definite decrease in electrical conductivity, but the temperature dependence is exponential.

In Fig.5.17 a diffractogram is shown for one of the studied layers of ZnO/ Sb_2O_3.

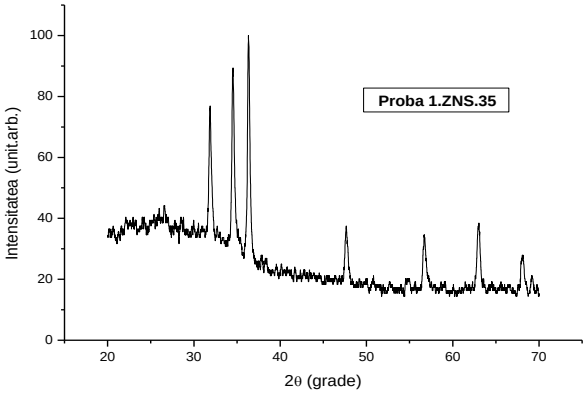

Fig.5.17 Diffractogram 1.ZNS.35 sample (thin layer of ZnO/ Sb_2O_3).

The XPS analysis established the presence of unoxidized Sb in the layers of Zn, which was not revealed by the diffraction pattern. The sample characteristics are presented in Table 5.1. In Fig.5.18 XPS spectrum is shown for one of the layers of Zn-doped Sb. It is noted the presence in the structure of antimony in the amorphous phase.

Table 5.1 Conditions for the preparation of thin films of ZnO:Sb.

Sample	*d* (nm)	Mass ratio Zn/Sb	T_{ox} (K)	t_{ox} (min)
7.ZNS.07	700	8/1	625	20
8.ZNS.08	800	8/2	625	30

d – layer thickness, T_{ox} – oxidation temperature, t_{ox} – oxidation time.

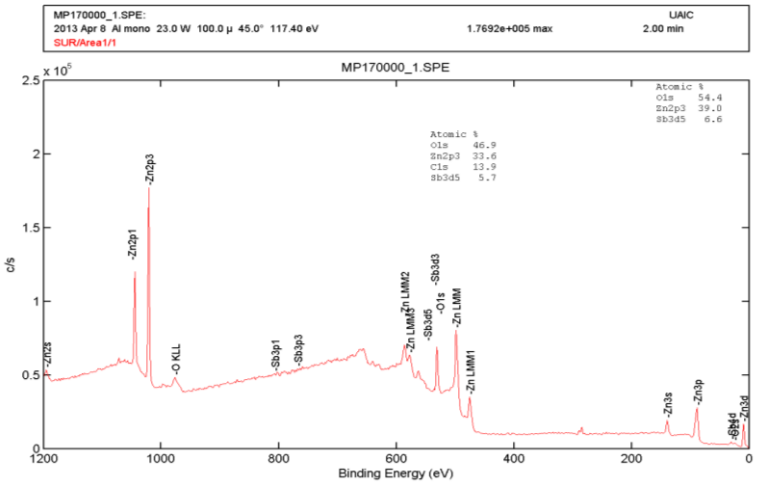

Fig.5.18 XPS spectrum for sample 7.ZNS.07 (Zn layer doped with Sb).

CONCLUSIONS

1. We prepared non-doped zinc oxide layers, others doped with Sb and Al. The trial was conducted in open atmosphere by thermal oxidation of thin layers of Zn, Zn-Sb and Zn-Al, submitted in advance by thermal vacuum evaporation.
   We have also prepared ZnO thin film by magnetron sputtering of the configuration, a mixture gas of argon and oxygen, and the target- Zinc disk.
2. If we analyze the two methods for the preparation of thin films, we can mention the following: (a) in both cases we are using vacuum systems, however, in the case of cathode spraying are required additional devices, specific to the phenomenon of the spraying (cathode, input devices gas pressure measuring site and its power source), (b) in the case of thermal oxidation are several ways to "interfere" in the preparation, that can determine the parameters of deposition and subsequent oxidation conditions; (c) trough spraying coating uniform layers are obtained, but the rate of deposition is relatively low (0.3 to 9.0 μm / h) in the case of the used system, (d) in each case, after deposition, heat treatments are required, in order to determine the structure of the layers and oxidize the remaining non-oxidized Zn atoms.
3. The structure and morphology of the layers were studied by X-ray diffraction (XRD), using the atomic force microscope (AFM). An assessment of the study was performed by XPS spectra.
   Investigations have shown that the ZnO thin films, prepared by the two methods, are polycrystalline and a Wurtz-type structure.
   ZnO layers with thickness d <1000 nm have crystallites preferentially oriented with the planes (002) parallel to the substrate surface. At greater thicknesses it is found the presence of crystallites with other orientations ((100), (101), (110), (103)).
   Unit cell parameters (hexagonal) of ZnO, determined on the basis of X-ray diffraction, have the values: a = 3.231 Å-3, 266 Å and c = 5.182 Å-5, 217 Å. They are very close to the standard values: a_0 = 3.2490 Å and c_0= 5.2066 Å.
4. For a large number of thin layers of ZnO we have determined a series of parameters of structure: the texture coefficient, mechanical stress and energy Zn-O bonds. The values found are discussed in the thickness of the layer and conditions of preparation.
   Crystallite size calculated by Debye-Scherrer equation, had values between 20 nm and 38 nm.
   AFM images can confirm that the ZnO layers are polycrystalline and the crystallites have a uniform distribution.

5. We have shown that a heat treatment cycle consisting of heating and successive cooling in the temperature range 300-600 K, stabilizes the structure of the layers, and the temperature dependence of the electrical conductivity is reversible.

   The temperature dependence of the electrical conductivity, measured by using standard cell surface, with aluminum electrodes, is exponential. Graphs $\ln\sigma=f(10^3/T)$ has a low slope portion (0.1-0.3 eV) in temperatures below 400 K and a large portion of the slope (1.0-2.0 eV) in the temperature range exceeding 450 K.
6. We explained the mechanism of electrical conduction for samples deposited, using the Seto model. Applying this model, we determined, through the study of addictions $\ln\sigma=f(10^3/T)$, capture state concentration (N_t=1,5·10^{13}-1,2·10^{14} cm^{-2}) and that state energy E_t=0,3-0,5 eV).

   Applying the Mayadas-Shatzkes model we determined that carriers scattering on crystallites limits causes a decrease in conductivity by 2-3 orders of magnitude.

   We found that the doped ZnO thin films with Sb have a structure of type Wurtz. Antimony is present in the amorphous phase and cause a decrease in electrical conductivity and transmission coefficient that is visible.
7. In the visible range (400 nm to 700 nm) the transmission coefficient of the investigated samples varies between 70% and 90%. Doped layers have lower transmission coefficient. We have drawn the absorption spectra of the sample on the basis of the transmission spectra. Assuming direct band-band transitions were determined that the band gap values ranging between 3.08 eV and 3.30 eV.

   For incident photon energies $h\nu<E_g$ we found an exponential dependence of the absorption coefficient, according by the Ulbrach law.
8. We studied the phenomenon of photoluminescence for temperatures of 78 K and 293 K. The photoluminescence spectra allowed us to assess positions traps.

   We analyzed the characteristics of photovoltaic modules based on thin films of ZnO. In this regard, we studied the mechanisms of generation / recombination and transport of nonequilibrium charge carriers in heterojunction ZnO/In_2O_3/InSe:Cd. We had the following findings: (a) InSe absorption band edge is determined by indirect transitions involving excitons, (b) the spectral characteristics of photocurrent has a maximum for $h\nu$=1,5 eV, (c) diffusion length for InSe is between 0.9 μm and 1.8 μm.

   We have drawn the XPS spectra for the samples of ZnO studied to determine their degree of oxidation.

SELECTED BIBLIOGRAPHY

[1] H.L. Hartnagel, A.L. Dawar, A.K. Jain, C. Jagadish, *Semiconducting Transparent Thin Films*, Institute of Physics Publishing, Bristol, 1995.

[13] F.C.M. Van Pol, F.R. Blom, Th.J.A. Popma, *Thin Solid Films*, 204 (1991) 349.

[18] G.I. Rusu, G.G. Rusu, *Bazele fizicii semiconductorilor*, Vol. I, Ed. Cermi, Iaşi, 2005.

[19] I. Pop, V. Niculescu, *Structura corpului solid (Metode fizice de studiu)*, Ed. Academiei RSR, Bucureşti, 1974.

[23] I. Licea, *Fizica metalelor*, Ed. Ştiinţifică şi Enciclopedică, Bucureşti, 1986.

[24] I. Spânulescu, *Fizica straturilor subţiri şi aplicaţiile acestora*, Ed.Stiinţifică, Bucureşti, 1975.

[30] N. Ţigău, V. Ciupină, G. Prodan, G.I. Rusu, E. Vasile, *J. Cryst. Growth*, 269 (2004) 392.

[44] I.I. Rusu, *Teză de doctorat*, Universitatea „Al.I. Cuza", Iaşi, 1998.

[46] I. Vascan, *Teză de doctorat*, Universitatea „Al.I. Cuza" Iaşi, 1986.

[48] I.I. Rusu, M. Smirnov, G.G. Rusu, A.P. Râmbu, G.I. Rusu, *International Journal of Modern Physics B*, 24 (31) (2010) 6079-6090.

[60] D. Mardare, *Straturi subţiri policristaline şi amorfe. Oxidul de titan*, Editura Politehnium, Iaşi, 2005.

[61] G.I. Rusu, *Semiconductori organici*, Ed. Tehnică, Bucureşti, 1980.

[70] J. Volger, *Phys. Rev.*, 9 (1950) 1023.

[71] R.L. Petritz, *Phys. Rev.*, 104 (1956) 1508.

[73] J.Y.W. Seto, *J. Appl. Phys.*, 46 (1975) 5247.

[74] G. Baccarani, B. Ricco, G. Spandini, *J. Appl. Phys.*, 49 (1978) 5565.

[78] R. Swanepoel, *J. Phys. E. Sci. Instrum.*, 17 (1984) 896.

[82] C. Baban, G.G. Rusu, I.I. Nicolaescu, G.I. Rusu, *J. Phys. Condens. Mater*. 12 (2000) 7687.

[103] D.I. Rusu, G.G. Rusu, D. Luca, *Structural Characteristics and Optical Properties of Thermally Oxidized Zinc Films*, *Acta Phys. Polonica A*, 119(6) (2011) 850.

[104] V. Chiricenco, M. Caraman, I.I. Rusu, C. Leontie, *J. Lumin.*, 101 (2003), 71-77.

[132] I.I. Rusu, D.I. Rusu, *On the electronic transport and optical Properties of polycristalline ZnO films*, First Conference on Advances in Optical Materials, Oct.2005, Arizona, SUA.

[141] I. Caraman, E. Cuculescu, M. Stamate, G. Lazăr, V. Nedeff, I. Lazăr, D.I. Rusu, *Transport Mechanism Analysis of Non-Equilibrium Charge Carrier in Heterojunctions with GaS-CdTe:Mn Thin Films*, Thin Solid Films 517 (2009), 2399-2402.

[147] F. Urbach, *Phys. Rev.*, 92 (1953), 1324.

PUBLISHED PAPERS

Published papers in ISI magazines

1.1 **D.I. Rusu**, G.G. Rusu, D. Luca, *Structural Characteristics and Optical Properties of Thermally Oxidized Zinc Films*, Acta Physica Polonica A, 119 (6), (2011) 850. **(AIS 2011: 0,11)**

1.2 E. Cuculescu, I. Evtodiev, I. Caraman, L. Leontie, V. Nedeff, **D.I. Rusu**, *Transport and generation–recombination mechanisms of nonequilibrium charge carriers in ZnO/In2O3/InSe:Cd heterojunctions*, Thin Solid Films, 519 (2011) 7356–7359. **(AIS 2011: 0,60)**

1.3 I. Evtodiev, I. Caraman, L. Leontie, **D.I. Rusu**, A. Dafinei, *Recombination luminescence and trap levels in undoped and Al-doped ZnO thin films on quartz and GaSe (0 0 0 1) substrates*, Materials Research Bulletin, 47 (3), 2012, 794-797. **(AIS 2012: 0,55)**

1.4 I.I. Rusu, **D.I. Rusu**, *Optical transmission and absorption of ZnO thin films*, Romanian Journal of Physics, vol. 43(1-2), 589, 1998.

1.5 I.I. Rusu, M. Caraman, **D.I. Rusu**, *Reflexion in the $\hbar\omega << E_g$ range for ZnO reactive sputtered films in planar magnetron*, Romanian Journal of Physics, 43(1-2), 153, 1998.

1.6 I. Caraman, G. Lazăr, L. Bibire, I. Lazăr, M. Stamate, **D.I. Rusu**, *The optical properties of Cd1-xMnxTe (0<x<0,55) solid solutions in monocrystals and thin polycrystalline films*, Physica Status Solidi C, No.6, vol. 5, 1203-1206 (2009). **(AIS 2011: 0,49)**

1.7 I. Caraman, I. Lazăr, M. Caraman, **D.I. Rusu**, *Surface structure of CdS layer at the interface of Cds-SnO_2 junction and the diagram of surface states*, Advanced Topics in Optoelectronics, Microelectronics and Nanotechnologies, Proc. SPIE, vol. 7297, 2009.

1.8 M. Stamate, G. Lazăr, V. Nedeff, I. Lazăr, I. Caraman, I. Rusu, **D.I. Rusu**, *The influence of Reactive Gaseous Flow Rate and Composition on the Optical Properties of TiO_2 Thin Films Deposited by DC Magnetron*, Acta Physica Polonica A, vol. 115 (3) (2009), 757. **(AIS 2011: 0,10)**

1.9 I. Caraman, E. Cuculescu, M. Stamate, G. Lazăr, V. Nedeff, I. Lazăr, **D.I. Rusu**, *Transport Mechanism Analysis of Non-Equilibrium Charge Carrier in Heterojunctions with GaS-CdTe:Mn Thin Films*, Thin Solid Films 517 (2009), 2399-2402. **(AIS 2011: 0,60)**

Article Influence Score (TOTAL): 2,45

Published papers in the University Annals

2.1 **D.I. Rusu**, I.I. Rusu, *On the thermoelectric properties of ZnO films prepared by DC magnetron sputtering*, MOCM 14. Volume 2, ROMANIAN TECHNICAL SCIENCES ACADEMY, 2008.

2.2 **D.I. Rusu**, I.I. Rusu**,** *The influence of heat treatment on the electrical conductivity of ZnO thin films*, Analele Ştiinţifice ale Universităţii "Al. I. Cuza" Iaşi, Tomul XLVI. S. Fizica Stării Condensate, (2000), p.113-118.

2.3 I. Caraman, M. Stamate, M. Caraman, **D.I. Rusu**, *The technique of measurement of modulated optical spectra*, Modelling and Optimization in the Machines Building Field, Romanian Technical Sciences Academy, (2) 2007, 104-107.

2.4 M. Caraman, G. Lazăr, I. Vascan, I. Lazăr, M. Stamate, I. Rusu, **D.I. Rusu**, *Absorbţia în domeniul vizibil a straturilor subţiri de carbon amorf hidrogenat*, Analele Ştiinţifice ale Universităţii de Stat din Moldova, 31-35, 2002.

Published papers at scientific events

3.1 **D.I. Rusu**, I.I. Rusu, *Asupra mecanismului conducţiei electrice în straturi subţiri semiconductoare de ZnO*, Sesiunea Ştiinţifică – Universitatea Bacău, 1996.

3.2 I.I. Rusu, I.D. Bursuc, **D.I. Rusu**, M. Caraman, I. Vascan, *Asupra transmisiei optice în straturi subţiri de ZnO obţinute prin pulverizare catodică în sistem magnetron*, Colocviul Naţional de Fizică, Chişinău, Rep. Moldova, 1997.

3.3 I.I. Rusu, I.D. Bursuc, **D.I. Rusu**, M. Caraman, I. Vascan, *Conductivitatea electrică a straturilor subţiri de ZnO obţinute prin pulverizare reactivă catodică în sistem magnetron circular*, Colocviul Naţional de Fizică, Chişinău, Rep. Moldova, 1997.

3.4 I.I. Rusu, I. Vascan, **D.I. Rusu**, M. Stamate, *IR reflection of ZnO thin films, The Third International Conference on Low Dimensional Structures and Devices*, 15-17 September 1999, Antalya, Turkey (p.12).

3.5 I.I. Rusu, **D.I. Rusu**, *Influenţa tratamentului termic asupra conductivităţii electrice a straturilor subţiri de ZnO*, Colocviul Naţional de Fizica şi Tehnologia Materialelor Amorfe, Iaşi, 8-11 Iunie, 2000.

3.6 I.I. Rusu, **D.I. Rusu**, *On the optical properties of ZnO films prepared by DC magnetron sputtering*, 7th International Conference of Advanced Materials, Iaşi, Iunie 2004.

3.7 I.I. Rusu, **D.I. Rusu**, *On the electronic transport and optical properties of polycristalline ZnO films*, First Conference on Advances in Optical Materials, Oct. 2005, Arizona, SUA.

3.8 I. Lazăr, I. Caraman, G. Lazăr, M. Stamate, I.I. Rusu, **D.I. Rusu**, *Preparation of C60 thin film by thermal vacuum evaporation*, Modelling and Optimization in the Machines Building Field, (3) 2007, 9-13.

3.9 I. Caraman, I. Lazăr, G. Lazăr, V. Nedeff, M. Stamate, I. Rusu, **D.I. Rusu**, *Nonlinear optical properties of C60 solutions*, 8th International Conference of Physics and Advanced Materials, Iaşi, 2008.

3.10 I. Caraman, E. Cuculescu, M. Stamate, G. Lazar, V. Nedeff, I. Lazar, **D.I. Rusu**, *Transport mechanism analysis of non-equilibrium charge carrier in heterojunctions with GaS-CdTe:Mn thin films*, E-MRS Strasbourg, May 2008.

3.11 M. Stamate, I. Lazăr, G. Lazăr, I. Caraman, N. Miron, D. Nistor, I. Rusu, **D.I. Rusu**, *AFM studies of TiO_2 thin films deposited through a DC magnetron sputtering method*, International Symposium on Applied Physics, 1st Edition, Galati, 2009.

3.12 I. Caraman, M. Stamate, I. Lazăr, G. Lazăr, **D.I. Rusu**, *FTIR spectroscopy applied to ceramical archaeological objects*, International Symposium on Applied Physics, 1st Edition, Galati, 2009.